MATHEMATICAL BIOSCIENCES
AND ENGINEERING
Volume **6**, Number **4**, October **2009**

doi:10.3934/mbe.2009.6.719

pp. **719–742**

SHARPNESS OF SATURATION IN HARVESTING AND PREDATION

Christopher M. Kribs-Zaleta

University of Texas at Arlington
Box 19408, Arlington, TX 76019-0408, USA

(Communicated by Yang Kuang)

Abstract. Harvesting and predation occur through contact processes in which the rate at which the managed (prey) population can be found depends on the population size, usually saturating at high densities. Many models incorporate saturation in this process without considering the effects of the particular function used to describe it. We show that the sharpness with which this saturation occurs has an important effect upon the resulting population dynamics, with bistability (sometimes involving a stable equilibrium and a stable limit cycle) occurring for saturation that is any sharper than the commonly used Michaelis-Menten (Holling type II) functional response. This sharpness threshold occurs across a wide range of model types, from simple harvesting to density-dependent and ratio-dependent predation.

1. **Saturation in harvesting and predation.** Harvesting and predation are both processes in which members of a population are removed by an external agency, sometimes for population management but more often for the benefit of the harvester, whether in the wild or in a managed environment. The two are distinguished in mathematical modeling by whether or not the harvester is dependent upon the yield (if the harvester or predator has other food sources, one develops a harvesting model that tracks only the harvested population; otherwise the model depicts a predator-prey system, in which the prey removal rate usually depends upon the predator population.) There is a long and extensive history of mathematical studies of both harvesting and predation, dating back most famously to Lotka and Volterra.

Both harvesting and predation normally take place through a so-called *contact process*; that is, the harvester or predator must come into contact with the prey, and the rate at which prey are removed increases with the frequency of these encounters, which increases in proportion to the size of each population. In predator-prey models, this contact rate is called the *predator functional response*. The predator functional response is commonly taken to be linear in the predator population density. Holling [11] famously classified the ways in which the contact rate may change with prey population density into a handful of types, each of which deals slightly differently with the fact that as prey become more plentiful, at some point the predators are satiated and predation (or harvesting) no longer increases (much). This corresponds to *saturation* in the contact process. In a Holling type I functional response, the harvesting rate increases linearly in the prey density until it reaches

2000 *Mathematics Subject Classification.* Primary: 92D25, 92D40; Secondary: 37G15.
Key words and phrases. saturation, predator-prey, harvesting, population biology, bistability.

the maximum level, at which point the increase cuts off abruptly, remaining constant for greater prey densities. We can also refer to this as a *switching model*, as the functional response, say $g(x) = H\min(x, A)$, switches over sharply from a linear increase to a constant rate once it reaches the maximum level H at prey density $x = A$. In a Holling type II functional response, generated by an assumption that increased prey handling time slows the harvesting, the saturation is more gradual, tapering off asymptotically as it approaches the maximum, typified by the smooth Verhulst [24] function $g(x) = Hx/(x + A)$ (also called Michaelis-Menten). Holling type III functional responses, typified by the Hill functions $g(x) = Hx^n/(x^n + A^n)$ for $n > 1$, represent opportunistic predation or harvesting, in which predation is very low below the threshold density A, above which it very rapidly approaches the maximum. Finally, some ecologists have extended this classification to a type IV functional response of the form $g(x) = HX/(A_0 + A_1x + x^2)$ to explore alternative assumptions about the predator attack rate. Thieme and Yang [23] considered a more complex saturation term in a predator-prey complex formation model.

Population harvesting models typically make one of two assumptions in modeling the rate at which individuals are removed from the population (e.g., [5]): One possibility, called *constant-effort harvesting* (CEH), holds that the effort expended in harvesting (the reciprocal of the average time until a given individual is removed) is constant, with the resulting harvesting rate being the product of the effort and the population size. Under this assumption, more individuals are removed per unit time when the population is large than when it is small, since it is much easier to find individuals for removal when the population is large. The alternative assumption, called *constant-yield harvesting* (CYH), holds that a certain (constant) number of individuals will be removed in unit time, regardless of population size or the effort required to remove them. Under this assumption, it is demand (harvest yield), rather than resources (harvest effort), that constrains the removal.

Each of these two assumptions may be accurate under different circumstances. In practice, regardless of the source or purpose of the harvesting in question, both resources and demand are likely to act as constraints; the question is which imposes the lower constraint. When the population is sufficiently large, the effort required to remove an individual is low enough that effort is no longer the dominant constraint, and the desired harvest yield can be met, leading to constant-yield harvesting. When the population is small enough, however (perhaps as a result of overharvesting), it becomes more difficult to find and remove a given individual, so that at some point the effort required to harvest the desired yield rate is greater than the maximum available effort, and the effort becomes the limiting constraint, leading to constant-effort harvesting. Imposing only one of these two constraints leads to unrealistic predictions in the corresponding model: the classical constant-yield harvesting model [5, 6] predicts extinction of the harvested population in finite time when overharvesting occurs, whereas in reality the desired harvesting yield is unsustainable once the population level is low—instead, the increase in required effort will reduce the yield before the population reaches extinction, even if the intent is to drive the population extinct. The classical constant-effort harvesting model [5, 22], on the other hand, predicts unrealistically high yields when the population is high (assuming that harvesting refers to physical removal of an individual).

We may form a more realistic model by incorporating both constraints, limiting harvest yield to a target level and limiting harvest effort to some maximum

available effort. Such a model must describe how the effective harvesting rate behaves in a neighborhood of the critical level where one constraint gives way to the other. Two recent studies [15, 16], which considered both sharp (Holling type I) and gradual (type II) saturation in rates such as this, found that the resulting model behavior may differ qualitatively depending on the sharpness of the saturation. In the following sections we introduce models in which a tuning parameter n controls the sharpness of the saturation, and we observe the effects of this parameter upon the harvested population, beginning with the simplest possible harvesting model and continuing on to observe parallels in the behavior of systems with conventional as well as ratio-dependent predation. We end with some conclusions about the thresholds exhibited in the saturation sharpness n.

2. **Saturation in the simplest harvesting model.** We consider first the simplest possible harvesting model, in which a single population $x(t)$ with a natural net growth rate of $f(x)$ undergoes harvesting at a rate $g(x)$ dependent on some combination of the population size and external factors (modeled through constant parameters). Hence $dx/dt = f(x) - g(x)$. We can also consider this as predation by predators with many other food sources. To give the population some robustness, we assume its natural growth is logistic, $f(x) = rx(1 - x/K)$, with intrinsic maximum per-capita growth rate r and carrying capacity K in the present environment. We assume that the maximum desired harvesting yield (removal rate) is H and the maximum available harvesting effort is $E_{max} = H/A$, with H as above and A the critical population level, above which yield is the dominant constraint and below which effort is the dominant constraint.

If we superimpose the two harvesting constraints, so that $g(x) \le H$ and also $g(x) \le E_{max}x$, then we arrive at the sharp (Holling type I) saturation model

$$\frac{dx}{dt} = rx\left(1 - \frac{x}{K}\right) - H\min\left(\frac{x}{A}, 1\right), \tag{1}$$

in which $g(x) = H\min(x/A, 1)$. Here A acts as a switching point between two submodels, the classical constant-yield harvesting (for $x > A$) and constant-effort harvesting (for $x < A$) models, whose behaviors are already well known. The CYH model has two equilibria,

$$x^*_{\pm} = \frac{1}{2}K\left(1 \pm \sqrt{1 - \frac{4H}{rK}}\right),$$

iff $H \le rK/4$, the larger of which is always locally asymptotically stable (henceforth LAS) when it exists, and the smaller of which is always unstable. If $H > rK/4$, there are no equilibria and the population goes extinct in finite time. Meanwhile, the CEH model has a zero (extinction) equilibrium which always exists, and is LAS iff $H \ge rA$ (i.e., $E_{max} \ge r$), and a positive equilibrium $K(1 - H/rA)$ that exists iff $H < rA$ ($E_{max} < r$) and is always LAS when it exists.

Equilibria from the CEH model for which $x^* < A$ will appear in the switching (sharp saturation) model, as will those from the CYH model for which $x^* > A$. The trivial equilibrium $E_0 = 0$ from the CEH model is thus always part of the switching model, while the positive equilibrium $E_1 = K\left(1 - \frac{H}{rA}\right)$ will appear iff it exists and $E_1 < A$, i.e., iff $H < rA$ and $H > rA\left(1 - \frac{A}{K}\right)$. The CYH equilibria $E_2 = x^*_+$ and $E_3 = x^*_-$, which exist when $H \le rK/4$, will appear in the switching model iff

$x_{\pm}^{*} > A$, which can be rewritten as

$$\pm\sqrt{1-\frac{4H}{rK}} > 2\,\frac{A}{K} - 1.$$

For E_2 this can be simplified to $K > 2A$ or $H < rA\left(1-\frac{A}{K}\right)$. For E_3 it can be simplified to $K > 2A$ and $H > rA\left(1-\frac{A}{K}\right)$. Since this model is a single, autonomous differential equation, whose solutions are monotone, we can extend local to global stability where there is a single asymptotically stable equilibrium.

We can simplify these expressions and reduce the number of parameters from four to two by defining

$$a = \frac{A}{K}, \quad h = \frac{H}{rK/4}.$$

Here, a recalibrates the switching point in terms of the carrying capacity, while h expresses the desired harvest yield in terms of the critical harvesting rate $rK/4$. The equilibria of the switching model (1) are given in terms of a and K in Table 1, with bifurcation diagrams in Figures 1 and 2[1].

As can be seen in the figures, there is a region of parameter space in which the model is bistable: to the left of the inverted parabola, E_2 competes with either E_0 or E_1, creating a hysteresis in which the same rate of harvesting can, in the former case, either wipe the population out asymptotically or leave it at a relatively high level, and in the latter case lead to either a low or high population level, with the unstable E_3 serving to separate the two basins of attraction in either case.

If, instead, we suppose that the harvesting rate saturates more smoothly as the effort constraint gives way to the demand constraint (as x increases), then we find no bistability between two positive equilibria. One common way to model a smooth transition from CEH to CYH is to use a Verhulst (Holling Type II) function, $g(x) = Hx/(x+a)$, leading to the harvesting model

$$\frac{dx}{dt} = rx\left(1-\frac{x}{K}\right) - H\,\frac{x}{x+A}. \tag{2}$$

Note that $Hx/(x+A) \leq H\min(x/A, 1)$ (with equality only at $x = 0$, and asymptotically as $x \to \infty$). Equation (2) has the trivial equilibrium $\tilde{E}_0$ ($x^* = 0$) and, if $h < (a+1)^2$, the two equilibria $\tilde{E}_2 > \tilde{E}_3$, for which

$$\frac{x^*}{K} = \frac{1}{2}\left(1-a \pm \sqrt{(1+a)^2-h}\right),$$

with a and h as above. Some algebra shows that $\tilde{E}_2 > 0$ iff, in addition, $a < 1$ or $h < 4a$, while $\tilde{E}_3 > 0$ iff $a < 1$ and $4a < h < (a+1)^2$. Standard techniques show that $\tilde{E}_0$ is LAS when $h > 4a$, while $\tilde{E}_2$ is always LAS when it exists, and $\tilde{E}_3$ is always unstable. Again, local stability extends to global when there is a unique asymptotically stable equilibrium. Bifurcation diagrams for (2) are given in Figures 3 and 4.

The qualitative difference between the behaviors of models (1) and (2) is that sharp saturation creates a region with two positive attractors, where a sufficiently large abrupt change in population size (a sudden influx or a natural disaster, for instance) can have lasting effects by pulling the population into the basin of attraction of a different equilibrium. The fact that this particular bistability exists for the sharp saturation model but not the smooth saturation model leads to the question

[1] All figures in this article except the first part of Figure 10 were generated in Mathematica.

TABLE 1. The equilibria of equation (1) and their existence and stability conditions

Eqm.	x^*/K value	Exists in submodel if	Appears in switching model if	LAS iff
E_0	0	always	always	$h > 4a$
E_1	$1 - \frac{h}{4a}$	$h < 4a$	$h > 4a(1-a)$	exists
E_2	$\frac{1}{2}\left(1 + \sqrt{1-h}\right)$	$h \le 1$	$a < \frac{1}{2}$ or $h < 4a(1-a)$	exists
E_3	$\frac{1}{2}\left(1 - \sqrt{1-h}\right)$	$h \le 1$	$a < \frac{1}{2}$ and $h > 4a(1-a)$	never

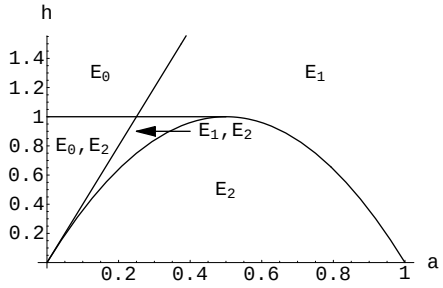

FIGURE 1. The a–h parameter plane divided into regions according to the stability of equilibria of model (1). In the two regions with bistability, E_3 exists as an unstable separatrix.

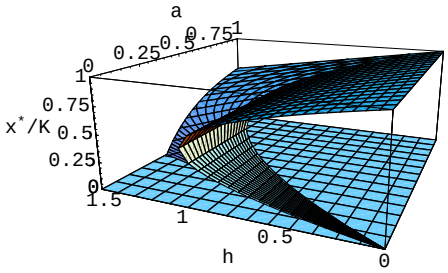

FIGURE 2. Bifurcation diagram for equation (1)

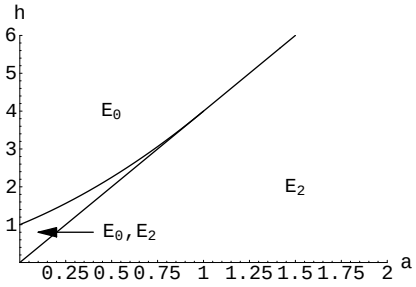

FIGURE 3. The a–h parameter plane divided into regions according to the stability of equilibria of model (2)

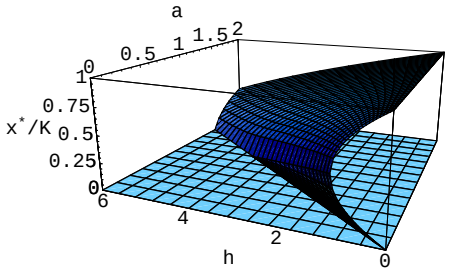

FIGURE 4. Bifurcation diagram for equation (2)

of how sharp the saturation in harvesting must be to create it. In the next section we consider precisely this question.

3. **A threshold in saturation sharpness.** As suggested in [15], one way to consider a progression of increasingly sharper saturation is to use the monotone sequence

$$g_n(x) = H\left(\frac{x^n}{x^n + A^n}\right)^{1/n},$$

of which the Verhulst function is the first ($n = 1$). (Note that $g_m(x) > g_n(x)$ when $m > n$ (and $x > 0$).) This gives us a spectrum of models

$$\frac{dx}{dt} = rx\left(1 - \frac{x}{K}\right) - H\frac{x}{\left(x^n + A^n\right)^{1/n}} \tag{3}$$

that saturate ever more sharply as n increases, with the saturation approaching Holling type I as $n \to \infty$. That is, n forms an abstract sharpness measure; high values of n imply that saturation occurs suddenly rather than gradually near the saturation point.

We can see immediately that $x^* = 0$ will always be an equilibrium of these models, and can show that its being LAS is independent of n:

$$\begin{aligned} f'(x) - g_n'(x) &= r\left(1 - \frac{2x}{K}\right) - H\frac{A^n}{\left(x^n + A^n\right)^{(1/n)+1}} \\ &= r\left[1 - 2\frac{x}{K} - \frac{h}{4}\frac{a^n}{\left(\left(\frac{x}{K}\right)^n + a^n\right)^{(1/n)+1}}\right], \end{aligned}$$

with h and a as defined in the previous section. For $x = 0$, this is $r(1 - h/4a)$, which is negative iff $h > 4a$. Thus the zero equilibrium is LAS for $h > 4a$, which was the case for both of the extremes studied in the previous section.

More generally, positive equilibria of (3) will be difficult to identify analytically, given the remaining equilibrium condition of order $2n$

$$F_n\left(\frac{x}{K}\right) := \left(1 - \frac{x}{K}\right)^n\left(\left(\frac{x}{K}\right)^n + a^n\right) - \left(\frac{h}{4}\right)^n = 0, \tag{4}$$

but we find that the behavior along the boundary of our parameter space is also independent of n. For $h = 0$, we have the simple logistic model with globally asymptotically stable (GAS) equilibrium $x^*/K = 1$, while for $a = 0$ the equation (3) has the equilibria

$$\frac{x^*}{K} = \frac{1}{2}\left(1 \pm \sqrt{1 - h}\right)$$

when $h \leq 1$. Since for $a = 0$ we have $f'(x) - g_n'(x) = r(1 - 2x/K)$, which is negative for $x^*/K > 1/2$, the greater of the two equilibria is always LAS, and the lesser unstable, acting (as in the previous section) as a separatrix between the basins (intervals) of attraction of the zero equilibrium and the greater positive equilibrium.

We can also observe the behavior along the line $h = 4a$, which is the only place where 0 is a root of F_n. We calculate

$$F_n(0) = a^n - \left(\frac{h}{4}\right)^n \quad \text{and} \quad F_n(1) = -\left(\frac{h}{4}\right)^n < 0,$$

so that $F_n(0) > 0 \Leftrightarrow h < 4a$, in which case there are an odd number (at least 1) of equilibria in (0,1), while above the line ($h > 4a$) there are an even number. In

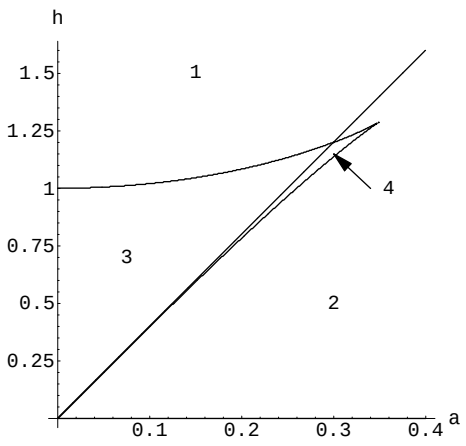

FIGURE 5. The a–h parameter plane divided into regions by the number of equilibria of model (3) with $n = 2$ (including the zero equilibrium)

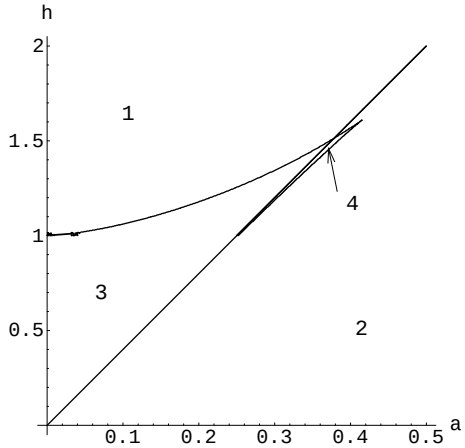

FIGURE 6. The a–h parameter plane divided into regions by the number of equilibria of model (3) with $n = 1.5$ (including the zero equilibrium)

particular, for $n > 1$, since $F_n'(0) = -na^n < 0$, the number of equilibria in (0,1) decreases by one as h increases past $4a$. For $n = 1$ we have $F_1'(0) = 1 - a$, so that as h increases past $4a$, the number decreases by one if $a > 1$ and increases by one if $a < 1$, as can be seen in Figure 3.

If we now juxtapose the fact that for all $n > 1$, the number of equilibria in (0,1) decreases by one as h increases past $4a$, with the facts that close to the a axis ($h \approx 0$, and below the line) that number is 1, while close to the h axis ($a \approx 0$, and above the line) that number is 2 for $h < 1$, we must conclude that there is another bifurcation curve, between either the a axis or the h axis and $h = 4a$, at which two equilibria appear. In fact, numerical explorations show that it is between the a axis and $h = 4a$, and that all models in the sequence (3) for which $n > 1$ behave qualitatively like the limiting ($n \to \infty$) case of sharp saturation (1). Figures 5 and 6 show the behavior for $n = 2$ and $n = 1.5$.

Since only the first of this sequence of models fails to exhibit a region of positive bistability, the question occurs as to whether the case $n = 1$ is truly a threshold case. To address this question, we can consider the index n to vary continuously rather than discretely. Further investigation shows that indeed it is: models of type (3) for which n is a noninteger greater than 1 behave just like those for which n is an integer greater than 1 (see Figure 6 for the picture with $n = 1.5$). On the other hand, models of this form for which $0 < n < 1$ have unbounded regions of survival-extinction bistability in the a-h plane separating the regions of globally asymptotically stable (henceforth GAS) survival and globally stable [asymptotic] extinction (see Figure 7 for the picture with $n = 0.5$). The case $n = 1$ therefore bridges the gap, exhibiting only one type of bistability as do the cases with $n < 1$ but with a bounded region of survival-extinction bistability like the cases with $n > 1$.

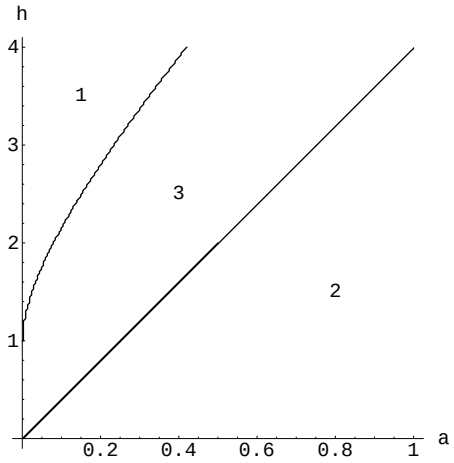

FIGURE 7. The a–h parameter plane divided into regions by the number of equilibria of model (3) with $n = 0.5$ (including the zero equilibrium)

In [16] a model is considered for the sylvatic transmission of the parasite *Trypanosoma cruzi*, which causes Chagas' disease, between host species such as raccoons and opossums and vector species such as *Triatoma sanguisuga*. In this transmission cycle, a predator-prey relationship is superimposed upon the host-vector interaction, as the hosts are opportunistic feeders which will eat insects when available, and there is evidence which supports this as an additional route of infection. Given the opportunistic nature of the predation, the host population is unaffected by it, but the prey is effectively subject to harvesting, with a variable effort such as that modeled by equations (1), (2), and (3). Because the infection's basic reproductive number R_0 is an increasing function of vector density, the existence of two locally stable vector densities (for sufficiently sharp saturation) presents the possibility that $R_0 < 1$ at the lower density but $R_0 > 1$ at the higher density, so that a one-time perturbation in vector density (such as that observed in Louisiana following Hurricane Katrina in 2005) can actually determine whether or not the infection cycle persists.

One may also ask whether there may be other saturation functions $g(x)$ besides the continuum described above. If we require only that $g(0) = 0$, g be nondecreasing, and $\lim_{x\to\infty} g(x) = H$, then certainly there are such functions (for example, the exponential functions $g_k(x) = H(1 - e^{-kx})$), but the property of interest, which generates the additional bistability, is the sharpness with which the saturation occurs. One measure of this sharpness is the curvature of the saturation function at the saturation point. The curvature of a function $g(x)$ at a particular point is given by

$$\kappa_g(x) = \frac{g''(x)}{\left[1 + (g'(x))^2\right]^{3/2}};$$

for the monotone sequence $g_n(x)$ defined above, we calculate

$$\kappa_{g_n}(x) = -\frac{H(n+1)A^n x^{n-1}\left(x^n + A^n\right)^{1+\frac{2}{n}}}{\left[H^2A^{2n} + \left(x^n + A^n\right)^{2+\frac{2}{n}}\right]^{3/2}}.$$

At the saturation point $x = A$, this becomes

$$\kappa_n := \kappa_{g_n}(A) = -\frac{H(n+1)2A4^{1/n}}{\left[H^2 + 4A^2\,4^{1/n}\right]^{3/2}}.$$

We can observe that $\kappa_n \to 0$ as $n \to 0$ while $\kappa_n \to \infty$ as $n \to \infty$; thus the continuum of models given in (3) represents all possible curvatures, and the threshold $n = 1$ established above is also representative.

To illustrate this principle, we consider one other spectrum of functions commonly used to describe saturation: the Hill functions

$$\tilde{g}_n(x) = H\,\frac{x^n}{x^n + A^n},$$

which describe Holling Type III (opportunistic) predation for $n > 1$. Rather than preserving the constant-effort asymptote at low densities as the Holling Type II functions do, the Hill functions preserve the saturation point A as a halfway point: $\tilde{g}_n(A) = H/2$. As $n \to 0$, $\tilde{g}_n(x)$ approaches the constant function $H/2$; as $n \to \infty$, $\tilde{g}_n(x)$ approaches a step function which switches from 0 to H at $x = A$. The Verhulst function again serves as the boundary case $n = 1$, between increasingly concave functions ($n < 1$) and increasingly sigmoid functions ($n > 1$). This class of models includes that proposed for the spruce budworm by Ludwig, Jones and Holling [18], who used $n = 2$.

If we consider the resulting harvesting models, $dx/dt = f(x) - \tilde{g}_n(x)$, we see that $x^* = 0$ is always an equilibrium (as long as $A > 0$), which is unstable for $n > 1$, LAS for $h > 4a$ if $n = 1$, and LAS for all h if $0 < n < 1$. Numerical investigation shows that for $0 < n < 1$ there are either 2 positive equilibria (one LAS, one unstable) or none, so that for relatively low harvest rates there is an Allee effect, while for relatively high harvest rates the population goes asymptotically extinct (see Figure 8). For $n > 1$, numerical analysis also shows a unique, GAS positive equilibrium for most combinations of a and h, but for some combinations near the lower h-axis there are 3 positive equilibria, 2 of them LAS (see Figure 9). Once again the Verhulst function $n = 1$ serves as a threshold for sharpness of saturation, even though the sharpness toward which the Hill functions tend as n increases involves an unlikely discontinuity from no harvesting to maximal harvesting at the switch point A. The principle continues to hold that saturation sharper than the Verhulst function causes an additional bistability not present with smoother saturation.

4. **Saturation in predation.** Predation can be seen as an extension of harvesting, in the sense that predators effectively engage in prey harvesting. Predators that have a wide range of prey or other food available may not be constrained in their growth by the availability of one prey species, in which case the predator-prey system decouples, with the predator population autonomous and the prey population dependent on the end state of the predator population. In such a scenario, the prey population can be modeled alone by a harvesting equation such as those considered in the previous section. In this section, we will consider the effect of sharpness of saturation on some classical [coupled] predator-prey models.

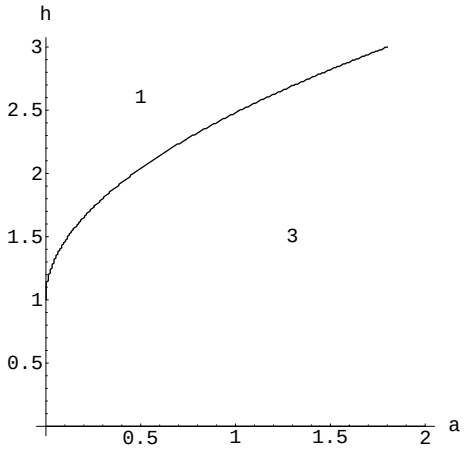

FIGURE 8. The a–h parameter plane divided into regions according to the number of equilibria for Hill-function harvesting with $n = 1/2$

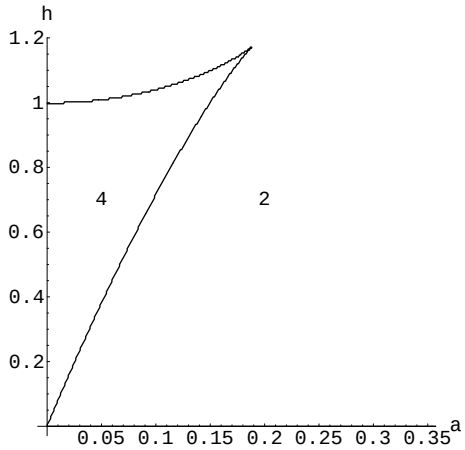

FIGURE 9. The a–h parameter plane divided into regions according to the number of equilibria for Hill-function harvesting with $n = 2$

Perhaps the most well known predator-prey system to incorporate saturation in predation (the Lotka-Volterra equations do not) is the Rosenzweig-MacArthur model [20] with logistic prey growth and Michaelis-Menten functional response (a.k.a. Holling type II or Verhulst),

$$\begin{aligned} \frac{dx}{dt} &= rx\left(1-\frac{x}{K}\right) - cy\,\frac{x}{x+A}, \\ \frac{dy}{dt} &= by\,\frac{x}{x+A} - dy, \end{aligned} \tag{5}$$

where x is the size of the prey population and y the size of the predator population. The first equation is an extension of the harvesting equation (2) with the maximum harvest rate $H = cy$ now given in terms of the predator population, with c the maximum predation rate per predator. The model assumes that predator population growth comes only from predation on this one prey, with conversion efficiency b/c and predator natural per capita mortality rate d. By assumption $b > d$, or else the predators would always go extinct. In this model (and the others studied later in this section) the saturation term implies that the prey are difficult to find at low densities ($x < A$).

This model has been extensively studied (e.g., [5, 9, 10, 12, 20, 21]); its behavior is summarized in Table 2, and depends on two parameters: the relative saturation point $a = A/K$ and the predator death-to-birth ratio $\delta = d/b < 1$. It has three equilibria: a double-extinction equilibrium $E_0(0,0)$, which is always unstable; a prey-only equilibrium $E_1(K,0)$, which is GAS for slow saturation (high a) and/or high death-to-birth ratio δ; and a coexistence equilibrium $E_2\left(\frac{\delta A}{1-\delta}, \frac{r}{c}\frac{A}{1-\delta}\left(1-\frac{a\delta}{1-\delta}\right)\right)$, which exists when E_1 is unstable and is GAS for intermediate values of a and δ.

For sufficiently low values of a and δ, there is a stable (attracting) limit cycle in which the predator population lags behind the prey in its ups and downs. (See Table 2 for specific criteria. Details of the analysis for this and other models in this section are given in the Appendix.)

If we sharpen the saturation in the functional response (predation terms), we obtain instead the following [Holling type I] model, originally studied by Dubois and Closset [7]:

$$\begin{aligned} \frac{dx}{dt} &= rx\left(1-\frac{x}{K}\right) - cy\min\left(\frac{x}{A},1\right), \\ \frac{dy}{dt} &= by\min\left(\frac{x}{A},1\right) - dy, \end{aligned} \tag{6}$$

which we can analyze by considering the two component systems. For $x < A$, we have $dx/dt = rx(1 - x/K) - (c/A)xy$, $dy/dt = (b/A)xy - dy$, which has again three equilibria: the unstable E_0; the prey-only E_1, which is GAS if $a\delta > 1$; and a slightly different coexistence equilibrium $\tilde{E}_2\left(\delta A, \frac{r}{c}A(1-a\delta)\right)$, which exists and is GAS if $a\delta < 1$. The LAS of the respective equilibria can be extended to GAS by the Poincaré-Bendixson Theorem after a straightforward application of Dulac's Criterion (with coefficient function $1/xy$) shows there are no closed trajectories in the interior of the positive quadrant.

The second component model of (6), in which $x > A$, is given by $dx/dt = rx(1 - x/K) - cy$, $dy/dt = by - dy$, which has no stable equilibria (E_0 and E_1 both exist but are unstable). Instead, the predator population grows exponentially without bound, $y(t) = y(0)\exp((b-d)t)$, eventually causing the prey population to decrease without bound. By itself, this system is ill-posed, in that the prey population becomes negative in finite time, but as a component of the switching model, it simply means that all trajectories will eventually be sent below the switching point $x = A$ to follow the dynamics of the first component model. The composite switching model (6) then has the two equilibria E_0 and E_1 common to both components, and in addition the equilibrium $\tilde{E}_2$ if it falls below the switch point. Simple calculation verifies that E_1 falls below the switch point whenever it is LAS, and that $\tilde{E}_2$ falls below the switch point whenever it exists. Likewise it is straightforward to verify that the two x-nullclines $y = (rA/c)(1 - x/K)$ and $y = (rx/c)(1 - x/K)$ coincide at $x = A$, while the first component's y-nullcline $x = \delta A$ always falls below the switch point and hence is incorporated into the model. The LAS of E_1 (if $a\delta > 1$) or $\tilde{E}_2$ (if $a\delta < 1$) can be extended to GAS for $a > 1$ ($A > K$) by considering the composite phase portrait and noting first that $dx/dt < 0$ above the switch point, so all trajectories end up below the switch point, where they remain, and where the local stability has already been extended to global.

For $a < 1$, however, numerical analysis indicates the presence of an additional bifurcation threshold $a = Q(\delta)$ not seen in system (5), above which $\tilde{E}_2$ is GAS, but below which it is only locally stable, surrounded by an unstable limit cycle, which is in turn surrounded by a stable limit cycle that is the attractor for the state space outside the unstable limit cycle. For δ fixed, as a decreases (i.e., as prey availability increases), $\tilde{E}_2$ enters the state space through E_1, becoming the global attractor, and then in crossing this additional threshold, away from the equilibrium there occurs a saddle-node bifurcation of limit cycles, in which the two limit cycles (verified analytically in [19]) appear. As a continues to decrease, the inner, unstable

TABLE 2. Summary of behavior for predator-prey models (5), (7) and (6)

Attractor(s)	Criterion for (5) (smooth saturation)	Criterion for (7) (intermediates)	Criterion for (6) (sharp saturation)
Limit cycle around E_2	$a < \dfrac{1-\delta}{1+\delta}$	$a < \delta^{n-1}\dfrac{(1-\delta^n)^{1/n}}{1+\delta^n}$	—
E_2 and limit cycle	—	$\delta^{n-1}\frac{(1-\delta^n)^{1/n}}{1+\delta^n} < a < Q_n(\delta)$	$a < Q(\delta)$
E_2 GAS	$\dfrac{1-\delta}{1+\delta} < a < \dfrac{1-\delta}{\delta}$	$Q_n(\delta) < a < \dfrac{(1-\delta^n)^{1/n}}{\delta}$	$Q(\delta) < a < 1/\delta$ (includes $a > 1$)
E_1 GAS	$a > \dfrac{1-\delta}{\delta}$	$a > \dfrac{(1-\delta^n)^{1/n}}{\delta}$	$a\delta > 1$

limit cycle approaches $\tilde{E}_2$, leaving the outer, stable limit cycle as the attractor for most initial conditions.

To examine the effects of a saturation that is intermediate in sharpness between the two extremes (5) and (6), we can again consider the model (5) with Verhulst-function saturation to be the first in a sequence of systems with increasingly sharp saturation:

$$\begin{aligned}\frac{dx}{dt} &= rx\left(1-\frac{x}{K}\right) - cy\frac{x}{(x^n+A^n)^{1/n}},\\ \frac{dy}{dt} &= by\frac{x}{(x^n+A^n)^{1/n}} - dy.\end{aligned} \tag{7}$$

System (7) has the three equilibria E_0 (always unstable), E_1 which is LAS iff $(a^n+1)\delta^n > 1$, and $\hat{E}_2$ given by

$$\left(\frac{\delta A}{(1-\delta^n)^{1/n}}, \frac{rA}{c(1-\delta^n)^{1/n}}\left(1-\frac{a\delta}{(1-\delta^n)^{1/n}}\right)\right),$$

which exists iff $a < (1-\delta^n)^{1/n}/\delta$ and is LAS iff

$$\delta^{n-1}\frac{(1-\delta^n)^{1/n}}{1+\delta^n} < a < \frac{(1-\delta^n)^{1/n}}{\delta}.$$

(Note that all these expressions approach the corresponding ones for system (6) as $n \to \infty$.) By eliminating the possibility of unbounded solutions as before, we can see that when no interior equilibrium exists E_1 must in fact be GAS. However, for $n > 1$ we again find the additional possibility, as in system (6), of bistability between $\hat{E}_2$ and a limit cycle. That is, numerical analysis confirms the existence for $n > 1$ of an additional threshold $a = Q_n(\delta)$, above which $\hat{E}_2$ is GAS, and below which $\hat{E}_2$ is surrounded by two limit cycles, respectively unstable and stable, as before. (For $n = 1$, $Q_1(\delta)$ coincides with the boundary $a = (1-\delta)/(1+\delta)$, so that the region does not exist. As $n \to \infty$, $Q_n(\delta) \to Q(\delta)$, the boundary for system (6).) In addition, there is the lower threshold given above, below which $\hat{E}_2$ is no longer stable. Numerical analysis indicates that at this lower threshold there is a Hopf bifurcation in which the unstable limit cycle merges with $\hat{E}_2$, leaving an unstable $\hat{E}_2$ surrounded by the outer limit cycle, which is still stable. Taken altogether, this phenomenon might be described as a "backward bifurcation of limit cycles" (see Figure 10).

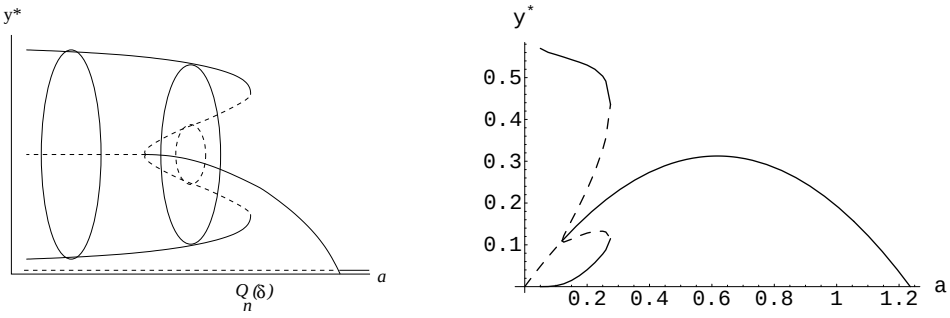

FIGURE 10. A bifurcation diagram for system (7) showing the three bifurcations in y^* as a varies. Left, an idealized version; right, the graph for $r = b = 1$, $c = 1$, $K = 1$, $\delta = 0.8$, $n = 10$.

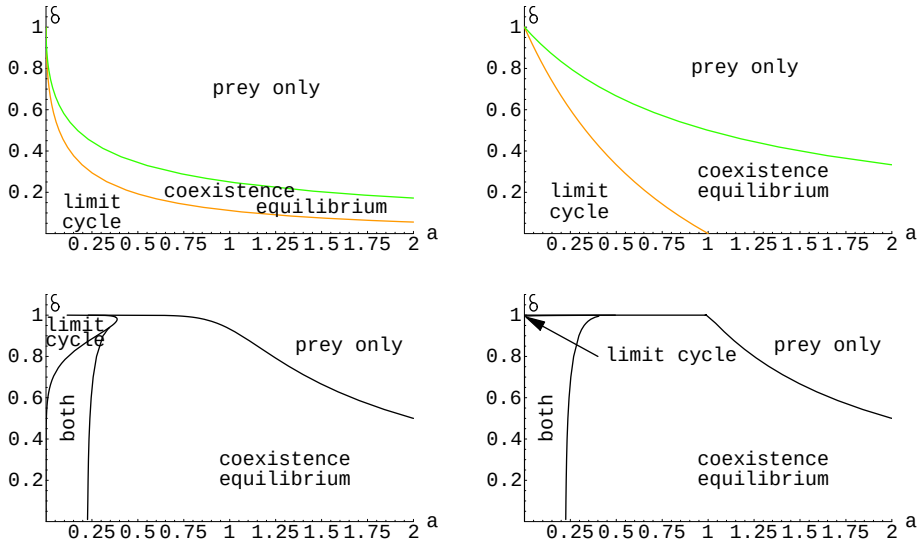

FIGURE 11. Effects of prey availability a and predator relative death rate δ on the behavior of the predator-prey system (7) for sharpness $n = 0.5,\ 1,\ 10,\ 1000$. "Both" denotes the region of bistability.

These results, as well as those for the limiting (sharp) saturation model, are also summarized in Table 2. The effects of the parameters a and δ are illustrated in Figure 11 for several values of the sharpness measure n. If we consider the entire spectrum of sharpness in predation saturation, we find that sharp ($n > 1$) saturation again causes bistability, in such a way that for some parameter values a sufficiently large perturbation away from a stable coexistence state can lead to sustained, and often large, oscillations (in fact, the smaller the perturbation needed, the larger the resulting oscillations).

In addition, sharper saturation favors predator survival: for $n > 1$ the predators survive unless prey are difficult to find even when plentiful (large a) and predators

live short lives ($\delta \approx 1$), and there are no persistent oscillations unless prey are easy to find even near extinction ($a \approx 0$) and again predators are short-lived. However, for smooth ($0 < n \leq 1$) saturation, predators will die out unless prey are easy to find even near extinction or the predators are exceptionally long-lived ($\delta \approx 0$).

Thus, while sharp saturation in prey harvesting for predators with multiple prey types available tends to encourage bistability of the prey population (which may not be in the predators' interest), sharp saturation in predation for predators with a single prey population tends to encourage bistability in *both* populations.

5. **Ratio-dependent predation.** Several authors (e.g., [1, 2, 14, 17]) have suggested that predation tends to saturate based not on the absolute density of the prey, but rather on the density of prey relative to predators, x/y, in cases where predators must search for prey. This assumption of ratio-dependent predation yields a saturation term of the form

$$\frac{x/y}{x/y + m}$$

for the number of prey caught per predator in unit time, where m is a half-saturation constant, the number of prey per predator at which predation reaches half its maximum rate. We can write this term more simply by multiplying top and bottom of the expression by y:

$$\frac{x}{x + my}.$$

In this form, known as the Michaelis-Menten-Holling type functional response [2, 14], we recognize the same saturation form we have been using, but with a half-saturation constant $A = my$ proportional to predator density. That is, the more predators there are, the higher the prey density must be before the prey are easy for predators to find (saturation).

It is important to note that the expression above which describes ratio-dependent predation is not only undefined at the origin but does not even have a well-defined limit there [14, 17]. The system can be defined piecewise as

$$\left(\frac{dx}{dt}, \frac{dy}{dt}\right) = \begin{cases} \left(rx\left(1 - \frac{x}{K}\right) - cy\,\frac{x}{x+my},\ by\,\frac{x}{x+my} - dy\right), & (x,y) \neq (0,0); \\ (0,0); & (x,y) = (0,0), \end{cases}$$

so that the derivatives are continuous at (0,0), since the per-capita predation term is bounded by 1 [25], but the system's behavior remains complex, including regions in parameter space for which some trajectories near the origin approach it asymptotically while others approach a coexistence equilibrium or a limit cycle; [4, 13, 25] gave complete descriptions of the resulting model's global dynamics.

To consider the effect of the sharpness in this saturation term on the dynamics of ratio-dependent predation, we pass directly to a model with variable sharpness n as in previous sections, taking $dx/dt = dy/dt = 0$ for $x = y = 0$, and otherwise

$$\begin{aligned} \frac{dx}{dt} &= rx\left(1 - \frac{x}{K}\right) - cy\,\frac{x}{\left(x^n + (my)^n\right)^{1/n}}, \\ \frac{dy}{dt} &= by\,\frac{x}{\left(x^n + (my)^n\right)^{1/n}} - dy. \end{aligned} \tag{8}$$

Although we will not be able to analyze this system's behavior near the origin using the Jacobian matrix, we will continue to refer to the asymptotic extinction of both populations as E_0. In addition, the system has two equilibria: the prey-only

equilibrium E_1 seen earlier, which is always an unstable saddle point for $0 < \delta < 1$ (allowing $\delta \geq 1$ here leads to predator extinction, with the prey sometimes surviving and sometimes not, depending on the initial prey-to-predator ratio [4, 25]), and the coexistence equilibrium $\check{E}_2(x^*, y^*)$, where

$$x^* = \left[1 - \alpha\left(1-\delta^n\right)^{1/n}\right] K, \quad y^* = \frac{\left(1-\delta^n\right)^{1/n}}{m\delta}\left[1 - \alpha\left(1-\delta^n\right)^{1/n}\right] K, \quad \alpha = \frac{c}{mr},$$

and $\delta = d/b < 1$ as before. $\check{E}_2$ exists when $\alpha\left(1-\delta^n\right)^{1/n} < 1$, and is LAS when

$$\alpha\left(1-\delta^n\right)^{1/n} < \min\left(1, \frac{1+\beta\delta(1-\delta^n)}{1+\delta^n}\right), \quad \text{with} \quad \beta = b/r.$$

Note that α is a dimensionless ratio of the maximum predation rate (per predator) to the product of the half-saturation constant and the prey growth rate; it is a measure of the relative intensity of predation.

The global behavior of system (8), like that of the well-studied case $n = 1$, can be complicated, with the origin E_0 acting as a saddle for $\alpha < 1$ (and $n \geq 1$), as the global attractor for $\alpha > 1/\left(1-\delta^n\right)^{1/n}$, and for intermediate values of α E_0 may have an attracting (stable node) sector and a repelling sector. A behavior that occurs only for $n > 1$, however, is a bistability between a LAS interior equilibrium and a stable limit cycle, as occurs in systems (6) and (7), through a backward bifurcation of limit cycles. We therefore see that the sharpness threshold remains the same ($n = 1$) whether predation is prey-dependent or ratio-dependent. (Details are again given in the Appendix, including explicit calculation of the first Lyapunov value using the approach given in [3].)

As sharpness of saturation increases ($n \to \infty$), the sequence of models in system (8) tends toward a piecewise linear limit in which the predation term is given by $y\min(x/my, 1)$, but we can simplify this and remove the singularity by rewriting it as $\min(x, my)/m$. This yields the switching model

$$\begin{aligned} \frac{dx}{dt} &= rx\left(1 - \frac{x}{K}\right) - \frac{c}{m}\min(x, my), \\ \frac{dy}{dt} &= \frac{b}{m}\min(x, my) - dy. \end{aligned} \tag{9}$$

This system has three equilibria: the double-extinction equilibrium E_0, which is globally stable when $\alpha = c/mr > 1$; the prey-only equilibrium E_1, which is always an unstable saddle; and the coexistence equilibrium $\bar{E}_2((1-\alpha)K, (1-\alpha)K/m\delta)$, which exists iff $\alpha < 1$ and is globally stable when it exists. (See Appendix for analysis.)

We see, therefore, that under sharp saturation the prey (and hence the predators) survive only when $\alpha < 1$: that is, when the prey's natural reproduction rate outpaces the maximum consumption rate of prey per predator measured in half-saturation units. It is significant to note that the complex behavior exhibited by system (8) is absent under completely sharp saturation, as both the existence of a stable sector for E_0 (observed for $n \geq 1$) and the equilibrium/limit cycle bistability (observed for $n > 1$) occur for intermediate intervals in α whose endpoints approach 1 asymptotically as $n \to \infty$, thus disappearing in the limiting case (9). However, the Holling type II saturation $n = 1$ again proves to be a threshold beyond which bistability can occur.

6. **Discussion.** Since mathematical models can at best approximate the behavior of real biological systems, and the specific functions used to represent observed characteristics are often chosen for mathematical simplicity and tractability rather than for close fits to detailed biological data, it is desirable to draw conclusions with robust support: that is, conclusions that follow from general qualitative assumptions about how populations develop, and hold true across a spectrum of specific models obeying those assumptions. Saturation in the contact processes that drive population management and predation is observed in real biological systems, but there is a continuum of sharpness with which that saturation can set in. The simple models explored in this paper all point to a sharpness threshold beyond which a common phenomenon occurs: bistability, either between two stable equilibria or between a stable equilibrium and a stable oscillation.

Historically, saturation in predation and harvesting has been considered to be either completely sharp (Holling type I) or smooth as typified by a Michaelis-Menten (Holling type II) functional response. The investigation in this paper consistently suggests that the degree of sharpness exhibited by the latter response is that threshold, and that any saturation even a little sharper than that can exhibit this bistability which could have serious consequences for the population(s) involved: Short-term fluctuations in the harvested (prey) population may result in sustained density changes or oscillations, which may also affect any predators involved which are dependent upon the prey. It may therefore be important to consider such "sharper" models, since the precise degree of sharpness with which these processes saturate (measured here by the parameter n) is not well known in general, and the sharper models—with sudden-onset, rather than gradual, saturation—allow the prediction of additional behaviors.

There remains work to do in following up these conclusions, including a more complete analysis of the conditions under which system (8) exhibits each of its possible behaviors, as well as the effects of sharpness of saturation in other harvesting and predation models. Also, some recent studies (e.g., [9, 16]) juxtapose infection in predator or prey species (or both) with the predation relationship, and even the cursory consideration mentioned in Section 3 indicates that the bistability caused by sharp saturation in predation can affect a disease's ability to invade. Finally, we recall that the study on saturation in contact processes that preceded the present work also suggests that other contact processes, such as infection itself, may be affected in similar ways [15].

Part of this research was conducted while visiting the University of Bordeaux. The author acknowledges Dr. Faina Berezovskaya of Howard University for a copy of [3] *as well as help interpreting it, Dr. Anuj Mubayi for help with references, and Dr. Christopher Hall of Berry College for a fruitful and ongoing collaboration which inspired the work related to* Trypanosoma cruzi. *The author also acknowledges support from a Norman Hackerman Advanced Research Program grant.*

This article is dedicated to Fred Brauer on the occasion of his 77th birthday.

REFERENCES

[1] R. Arditi and L. R. Ginzburg, *Coupling in predator-prey dynamics: Ratio-dependence*, J. Theor. Biol., **139** (1989), 311–326.

[2] M. Bandyopadhyay and J. Chattopadhyay, *Ratio-dependent predator-prey model: Effect of environmental fluctuation and stability*, Nonlinearity, **18** (2005), 913–936.

[3] N. N. Bautin and E. A. Leontovich, "Methods and Tools of Qualitative Analysis of Planar Dynamical Systems" (in Russian), Nauka, Moscow, 1976.
[4] F. Berezovskaya, G. Karev and R. Arditi, *Parametric analysis of the ratio-dependent predator-prey model*, J. Math. Biol., **43** (2001), 221–246.
[5] Fred Brauer and Carlos Castillo-Chávez, "Mathematical Models in Population Biology and Epidemiology," Springer, New York, 2001.
[6] Fred Brauer and David A. Sánchez, *Constant rate population harvesting: Equilibrium and stability*, Theor. Pop. Biol., **8** (1975), 12–30.
[7] D. M. Dubois and P. L. Closset, *Patchiness in primary and secondary production in the Southern Bight: A mathematical theory*, in "Proceedings of the 10th European Symposium on Marine Biology, Ostend, Belgium, Sept. 17-23, 1975: Vol. **2**. Population Dynamics of Marine Organisms in Relation with Nutrient Cycling in Shallow Waters" (eds. G. Persoone and E. Jaspers), Belgium Universal Press, Wetteren, (1976), 211–229.
[8] H. I. Freedman, *Stability analysis of a predator-prey system with mutual interference and density-dependent death rates*, Bull. Math. Biol., **41** (1979), 67–78.
[9] Frank M. Hilker and Kirsten Schmitz, *Disease-induced stabilization of predator-prey oscillations*, Journal of Theoretical Biology, **255** (2008), 299–306.
[10] Josef Hofbauer and Karl Sigmund, "Evolutionary Games and Population Dynamics," Cambridge University Press, New York, 1998.
[11] C. S. Holling, *The functional response of predators to prey density and its role in mimicry and population regulations*, Mem. Entomol. Soc. Can., **45** (1965), 3–60.
[12] S. B. Hsu, S. P. Hubbell and P. Waltman, *Competing predators*, SIAM J. Applied Math., **35** (1978), 617–625.
[13] S. B. Hsu, T. W. Hwang and Y. Kuang, *Global analysis of the Michaelis-Menten-type ratio-dependent predator-prey system*, J. Math. Biol., **42** (2001), 489–506.
[14] C. Jost, O. Arino and R. Arditi, *About deterministic extinction in a ratio-dependent predator-prey model*, Bull. Math. Biol., **61** (1999), 19–32.
[15] C. M. Kribs-Zaleta, *To switch or taper off: The dynamics of saturation*, Math. Biosci., **192** (2004), 137–152.
[16] Christopher Kribs-Zaleta, *Vector consumption and contact process saturation in sylvatic transmission of T. cruzi*, Mathematical Population Studies, **13** (2006), 135–152.
[17] Y. Kuang and E. Beretta, *Global qualitative analysis of a ratio-dependent predator-prey system*, J. Math. Biol., **36** (1998), 389–406.
[18] D. Ludwig, D. D. Jones and C. S. Holling, *Qualitative analysis of insect outbreak systems: The spruce budworm and forest*, Journal of Animal Ecology, **47** (1978), 315–332.
[19] Y. Ren and L. Han, *The predator prey model with two limit cycles*, Acta Mathematicae Applicatae Sinica (English Series), **5** (1989), 30–32.
[20] M. L. Rosenzweig and R. H. MacArthur, *Graphical representation and stability conditions for predator-prey interactions*, American Naturalist, **97** (1963), 209–223.
[21] M. L. Rosenzweig, *Why the prey curve has a hump*, American Naturalist, **103** (1969), 81–87.
[22] M. B. Schaefer, *Some aspects of the dynamics of populations important to the management of commercial marine fisheries*, Bull. Inter-Amer. Trop. Tuna Comm., **I** (1954), 25–56.
[23] Horst R. Thieme and Jinling Yang, *On the complex formation approach in modeling predator prey relations, mating, and sexual disease transmission*, Electronic J. Diff. Eqns. Conf., **5** (2000), 255–283.
[24] P. F. Verhulst, *Notice sur la loi que la population suit dans son accroissement*, Corr. Math. et Phys., **10** (1838), 113–121.
[25] D. Xiao and S. Ruan, *Global dynamics of a ratio-dependent predator-prey system*, J. Math. Biol., **43** (2001), 268–290.

Appendix. Analysis for predation models.

System (5). For system (5) the prey nullclines are $x = 0$ and $y = \frac{r}{c}(1-x/K)(x+A)$, and the predator nullclines are $y = 0$ and $x = \delta A/(1-\delta)$. Prey and predator nullclines intersect at the three equilibria E_0, E_1 and E_2. A local stability analysis using standard techniques (e.g., the Jacobian matrix and the Routh-Hurwitz criteria) shows that E_0 is unstable, E_1 is LAS iff $(1+a)\delta > 1$, and E_2 is LAS iff $\frac{1-\delta}{1+\delta} < a < \frac{1-\delta}{\delta}$. The stability of the interior equilibrium E_2 can also be shown via

the graphical method of Rosenzweig and MacArthur [8, 20] by observing that the predator nullcline is vertical there, while the prey nullcline (a quadratic with roots at $x = -A$, $x = K$) is decreasing to the right of the vertex $x = \frac{K-A}{2}$, so that E_2 is LAS iff $\delta A/(1-\delta)$ falls to the right of $\frac{K-A}{2}$ (this condition can be simplified as given above).

To attend to global behavior issues, we first rule out unbounded solutions. We observe that $\frac{d}{dt}(bx+cy) = brx(1-x/K) - cdy < 0 \Leftrightarrow y > \frac{br}{cd}\,x(1-x/K)$ and then find a constant k such that $bx + cy > k \Rightarrow y > \frac{br}{cd}\,x(1-x/K)$. We do this by matching $dy/dx = -b/c = \frac{br}{cd}\,(1-2x/K)$, which yields $x = \frac{K}{2}\left(1+\frac{d}{r}\right)$, making $y = \frac{K}{4}\,\frac{br}{cd}\left(1-\frac{d^2}{r^2}\right)$. Thus

$$bx + cy = k = \frac{K}{4}\,\frac{br}{d}\left(1+\frac{d}{r}\right)^2.$$

Hence all solutions of (5) which begin with $bx + cy > k$ eventually pass below the line $bx + cy = k$, and any solutions for which $bx + cy < k$ remain inside the triangle $\{x \geq 0, y \geq 0, bx + cy < k\}$ thereafter. Now, for sufficiently high a and δ ($(a+1)\delta > 1$) E_2 does not exist, so there are no interior equilibria, and hence (by Poincaré-Bendixson) no limit cycles. Thus the LAS E_1 is in fact GAS. For sufficiently low a and δ ($a < (1-\delta)/(1+\delta)$) there are no stable equilibria, and thus (by Poincaré-Bendixson) all solutions must approach a periodic orbit. For intermediate values of a and δ, the LAS E_2 is in fact GAS (the proof, which applies Dulac's Criterion with a coefficient function of $\left(\frac{x}{x+A}\right)^M y^N$ for suitable values of M and N, is given in [12], Lemma 4.4 and [10], Theorem 4.4.3).

System (6). For the first ($x < A$) component of (6), equilibrium conditions require $x^* = 0$ or $y^* = (Ar/c)(1 - x^*/K)$, and $y^* = 0$ or $x^* = \delta A$. The resulting combinations yield E_0, E_1, and $\tilde{E}_2$ as given in the main text. The corresponding Jacobian matrix is

$$J = \begin{bmatrix} r\left(1-2\frac{x^*}{K}\right) - \frac{cy^*}{A} & -\frac{cx^*}{A} \\ \frac{by^*}{A} & \frac{bx^*}{A} - d \end{bmatrix},$$

from which we calculate $J(E_0) = \mathrm{diag}[r, -d]$,

$$J(E_1) = \begin{bmatrix} -r & -\frac{c}{a} \\ 0 & b\left(\frac{1}{a}-\delta\right) \end{bmatrix}, \text{ and } J(\tilde{E}_2) = \begin{bmatrix} -ra\delta & -c\delta \\ \frac{br}{c}(1-a\delta) & 0 \end{bmatrix}.$$

Thus E_0 is unstable, E_1 is LAS iff $a\delta > 1$, and $\tilde{E}_2$ is always LAS when it exists, since $\mathrm{tr}J(\tilde{E}_2) = -ra\delta < 0$, and $\det J(\tilde{E}_2) = rd(1-a\delta) > 0$ when $a\delta < 1$.

The second ($x > A$) component of the switching model has equilibrium conditions $y^* = (r/c)x^*(1-x^*/K)$ and $y^* = 0$, yielding only the equilibria E_0 and E_1, both of which can been seen to be unstable from the Jacobian matrix,

$$J = \begin{bmatrix} r\left(1-2\frac{x^*}{K}\right) & -c \\ 0 & b-d \end{bmatrix},$$

since the second eigenvalue $b - d > 0$ by assumption.

The composite model includes the first component's sometimes-stable E_1, rather than the second component's never-stable E_1, when its x^* value falls below the switch point, $K < A$ (i.e., $a > 1$). But this criterion is implied by the LAS criterion

$a\delta > 1$ since $\delta < 1$, so whenever $a\delta > 1$ it is the LAS E_1 that appears in the composite model (6).

Global behavior of each component, as well as of the composite model, is addressed in the main text.

System (7). Equilibrium conditions for (7) require $x^* = 0$ or $y^* = (r/c)(1 - x^*/K)(x^{*n} + A^n)^{1/n}$, and $y^* = 0$ or $x^* = \delta A/(1-\delta^n)^{1/n}$. Combinations yield E_0, E_1 and $\hat{E}_2$ as in the main text; LAS analysis uses the Jacobian matrix

$$J = \begin{bmatrix} r\left(1 - 2\frac{x^*}{K}\right) - \frac{cy^*A^n}{(x^{*n}+A^n)^{1+\frac{1}{n}}} & -\frac{cx^*}{(x^{*n}+A^n)^{1/n}} \\ \frac{by^*A^n}{(x^{*n}+A^n)^{1+\frac{1}{n}}} & b\left(\frac{x^*}{(x^{*n}+A^n)^{1/n}} - \delta\right) \end{bmatrix},$$

from which we calculate

$$J(E_0) = \begin{bmatrix} r & 0 \\ 0 & -d \end{bmatrix}, \quad J(E_1) = \begin{bmatrix} -r & -\frac{c}{(1+a^n)^{1/n}} \\ 0 & b\left(\frac{1}{(1+a^n)^{1/n}} - \delta\right) \end{bmatrix},$$

and

$$J(\hat{E}_2) = \begin{bmatrix} r\delta\left[\delta^{n-1} - a\frac{1+\delta^n}{(1-\delta^n)^{1/n}}\right] & -c\delta \\ \frac{br}{c}(1-\delta^n)\left(1 - \frac{a\delta}{(1-\delta^n)^{1/n}}\right) & 0 \end{bmatrix}.$$

Thus by inspection E_0 is unstable, and E_1 is LAS iff $\delta > 1/(1+a^n)^{1/n}$; i.e., $a > (1-\delta^n)^{1/n}/\delta$. The conditions for $\hat{E}_2$ to be LAS are

$$\mathrm{tr}J(\hat{E}_2) = r\delta\left[\delta^{n-1} - a\frac{1+\delta^n}{(1-\delta^n)^{1/n}}\right] < 0 \Leftrightarrow a > \delta^{n-1}\frac{(1-\delta^n)^{1/n}}{1+\delta^n} \text{ and}$$

$$\det J(\hat{E}_2) = rd(1-\delta^n)\left(1 - \frac{a\delta}{(1-\delta^n)^{1/n}}\right) > 0 \Leftrightarrow a < \frac{(1-\delta^n)^{1/n}}{\delta}.$$

System (8). The equilibrium conditions are

$$(x - \text{nullclines}) \quad \frac{dx}{dt} = 0 \quad \Leftrightarrow \quad x = 0 \text{ or } r\left(1 - \frac{x}{K}\right) = \frac{cy}{[x^n + (my)^n]^{1/n}},$$

$$(y - \text{nullclines}) \quad \frac{dy}{dt} = 0 \quad \Leftrightarrow \quad y = 0 \text{ or } \frac{bx}{[x^n + (my)^n]^{1/n}} = d.$$

To the double-extinction equilibrium $E_0(0,0)$ we add the two equilibria $E_1(K,0)$ and $\check{E}_2(x^*, y^*)$, where

$$x^* = \left[1 - \alpha\left(1-\delta^n\right)^{1/n}\right]K, \quad y^* = \frac{\left(1-\delta^n\right)^{1/n}}{m\delta}\left[1 - \alpha\left(1-\delta^n\right)^{1/n}\right]K,$$

$\alpha = c/mr$, and $\delta = d/b < 1$. Note $\check{E}_2$ exists when $\alpha < 1/\left(1-\delta^n\right)^{1/n}$.

The Jacobian matrix for the system is

$$J = \begin{bmatrix} r\left(1 - 2\frac{x}{K}\right) - cy\frac{(my)^n}{[x^n+(my)^n]^{1+\frac{1}{n}}} & -cx\frac{x^n}{[x^n+(my)^n]^{1+\frac{1}{n}}} \\ by\frac{(my)^n}{[x^n+(my)^n]^{1+\frac{1}{n}}} & bx\frac{x^n}{[x^n+(my)^n]^{1+\frac{1}{n}}} - d \end{bmatrix}.$$

Deferring for the moment the question of behavior near E_0, we find

$$J(E_1) = \begin{bmatrix} -r & -c \\ 0 & b-d \end{bmatrix},$$

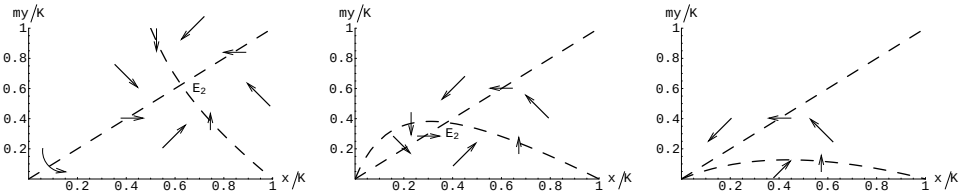

FIGURE 12. Phase portraits for system (8): from left to right, (a) $\alpha \leq 1$, (b) $1 < \alpha < 1/(1-\delta^n)^{1/n}$, (c) $\alpha > 1/(1-\delta^n)^{1/n}$. x-nullclines occur at $x = 0$ ($y > 0$) and $my = x(1 - x/K)/[\alpha^n - (1-x/K)^n]^{1/n}$; y-nullclines occur at $y = 0$ ($x > 0$) and $my = x(1-\delta^n)^{1/n}/\delta$. Note that in any case x is bounded by K, so y is bounded by $K(1-\delta^n)^{1/n}/m\delta$.

making E_1 an [unstable] saddle (since $b > d$ by assumption), and

$$J(\check{E}_2) = \begin{bmatrix} r\left(1 - 2\frac{x^*}{K}\right) - \frac{cy^*}{[x^{*n}+(my^*)^n]^{1/n}}(1-\Delta) & -\frac{c}{b}\frac{bx^*}{[x^{*n}+(my^*)^n]^{1/n}}\Delta \\ \frac{b}{c}\frac{cy^*}{[x^{*n}+(my^*)^n]^{1/n}}(1-\Delta) & \frac{bx^*}{[x^{*n}+(my^*)^n]^{1/n}}\Delta - d \end{bmatrix}$$

where $\Delta = x^{*n}/(x^{*n} + (my^*)^n)$. Using the equilibrium conditions, we can simplify this to

$$\begin{aligned} J(\check{E}_2) &= \begin{bmatrix} r\left(1 - 2\frac{x^*}{K}\right) - r\left(1 - \frac{x}{K}\right)(1-\delta^n) & -\frac{c}{b}\,d\,\delta^n \\ \frac{b}{c}\,r\left(1-\frac{x}{K}\right)(1-\delta^n) & d\,\delta^n - d \end{bmatrix} \\ &= \begin{bmatrix} r\left[\alpha(1-\delta^n)^{1/n}(1+\delta^n) - 1\right] & -c\delta^{n+1} \\ \frac{b}{m}(1-\delta^n)^{1+\frac{1}{n}} & -b\delta(1-\delta^n) \end{bmatrix}. \end{aligned}$$

The conditions for $\check{E}_2$ to be LAS are thus

$$\mathrm{tr}J(\check{E}_2) = r\left[\alpha(1-\delta^n)^{1/n}(1+\delta^n) - 1\right] - b\delta(1-\delta^n) < 0 \Leftrightarrow \alpha < \frac{1+\beta\delta(1-\delta^n)}{(1+\delta^n)(1-\delta^n)^{1/n}} \tag{10}$$

$$\text{and} \quad \det J(\check{E}_2) = br\delta(1-\delta^n)\left(1 - \alpha(1-\delta^n)^{1/n}\right) = br\delta(1-\delta^n)\frac{x^*}{K} > 0.$$

(As in the main text, $\beta = b/r$.) The latter condition is always satisfied when $\check{E}_2$ exists, so the additional criterion comes from the trace.

We now consider the system's behavior near E_0 using a phase portrait analysis, with three cases in α illustrated in Figure 12. (Note that in each case, solutions approach E_0 along the y-axis but go away from it, and toward E_1, along the x-axis.) For $\alpha < 1$, $n \geq 1$ (Figure 12(a)), E_0 acts like a saddle point and is not an attractor. We can see this by the following argument (cf. Theorem 2.2 in [17]): Consider the rescaled system

$$u' = u(1-u) - \alpha v\frac{u}{(u^n+v^n)^{1/n}}, \quad v' = \beta v\left[\frac{u}{(u^n+v^n)^{1/n}} - \delta\right], \tag{11}$$

where $u = x/K$, $v = my/K$, and time has been rescaled to eliminate r. $u' > u[(1-\alpha) - u]$, so $u(t) > \phi(t)$ where $\phi' = \phi[(1-\alpha) - \phi]$ and $\phi(0) = u(0)$. Thus

$\liminf_{t\to\infty} u(t) \geq \lim_{t\to\infty} \phi(t) = 1-\alpha > 0$. Therefore for some time T, $u(t) > (1-\alpha)/2$ for all $t > T$. Then, for $t > T$,

$$v' > \beta v \left[\frac{\left(\frac{1-\alpha}{2}\right)}{\left(\left(\frac{1-\alpha}{2}\right)^n + v^n\right)^{1/n}} - \delta \right] \geq \beta v \left[\frac{\left(\frac{1-\alpha}{2}\right)}{\left(\frac{1-\alpha}{2}\right) + v} - \delta \right],$$

with the second inequality following from the fact that $u/(u^n+v^n)^{1/n}$ is increasing in n (for fixed $u, v > 0$). Then $v(t) > \psi(t)$ where

$$\psi' = \beta\psi \left[\frac{\left(\frac{1-\alpha}{2}\right)}{\left(\frac{1-\alpha}{2}\right) + \psi} - \delta \right], \quad \psi(0) = v(0),$$

and $\liminf_{t\to\infty} v(t) \geq \lim_{t\to\infty} \psi(t) = \frac{1-\delta}{\delta}\frac{1-\alpha}{2} > 0$. Hence system (8) is permanent.

For $\alpha > 1/(1-\delta^n)^{1/n}$ (Figure 12(c)), E_0 is the global attractor, as can be seen by an argument identical to that in Theorem 2.6 of [17] and that given in more detail for system (9) in the next section, namely an inevitable, irreversible counterclockwise progression from one region of the phase portrait to the next.

For $1 < \alpha < 1/(1-\delta^n)^{1/n}$ (Figure 12(b)), there is the possibility for E_0 to have an attracting (stable node) sector when $n \geq 1$, in the case that $\alpha > 1+\beta\delta$; this can be seen by adapting the proofs of Theorems 2.3 and 2.4 in [17] (given there for $n = 1$) in a similar way to that done above for $\alpha < 1$.

Finally, with regard to global behavior when E_0 is not the sole attractor (i.e., when $\check{E}_2$ exists), we can verify the equilibrium/limit cycle bistability by computing the first Lyapunov value [3] at the Hopf bifurcation, which occurs when $\mathrm{tr}J(\check{E}_2) = 0$. This requires translating $\check{E}_2$ to the origin and Taylor-expanding to obtain terms up to third-order: if $x' = f(x,y)$, $y' = g(x,y)$, then we write $x = x^* + \tilde{x}$, $y = y^* + \tilde{y}$ and expand, writing the Taylor series (centered at $(x,y) = (x^*, y^*)$, i.e., $(\tilde{x}, \tilde{y}) = (0,0)$):

$$\begin{aligned}
\tilde{x}' = x' = f(x^*+\tilde{x}, y^*+\tilde{y}) =& a_{10}\tilde{x} + a_{01}\tilde{y} + a_{20}\tilde{x}^2 + a_{11}\tilde{x}\tilde{y} + a_{02}\tilde{y}^2 \\
&+ a_{30}\tilde{x}^3 + a_{21}\tilde{x}^2\tilde{y} + a_{12}\tilde{x}\tilde{y}^2 + a_{03}\tilde{y}^3 + \mathcal{O}(4), \\
\tilde{y}' = y' = g(x^*+\tilde{x}, y^*+\tilde{y}) =& b_{10}\tilde{x} + b_{01}\tilde{y} + b_{20}\tilde{x}^2 + b_{11}\tilde{x}\tilde{y} + b_{02}\tilde{y}^2 \\
&+ b_{30}\tilde{x}^3 + b_{21}\tilde{x}^2\tilde{y} + b_{12}\tilde{x}\tilde{y}^2 + b_{03}\tilde{y}^3 + \mathcal{O}(4).
\end{aligned}$$

Then we calculate the first Lyapunov value L_1 as follows:

$$\begin{aligned}
L_1 = -\frac{\pi}{4a_{01}\omega^3} \Big\{ & \big[a_{10}b_{10}(a_{11}^2 + a_{11}b_{02} + a_{02}b_{11}) + a_{10}a_{01}(b_{11}^2 + b_{11}a_{20} + b_{20}a_{11}) \\
& + b_{10}^2(a_{11}a_{02} + 2a_{02}b_{02}) - a_{01}^2(b_{11}b_{20} + 2a_{20}b_{20}) - 2a_{10}b_{10}(b_{02}^2 - a_{20}a_{02}) \\
& - 2a_{10}a_{01}(a_{20}^2 - b_{20}b_{02}) + (a_{01}b_{10} - 2a_{10}^2)(b_{11}b_{02} - a_{11}a_{20})\big] \\
& - (a_{10}^2 + a_{01}b_{10})\left[3(b_{10}b_{03} - a_{01}a_{30}) + 2a_{10}(a_{21} + b_{12}) + (b_{10}a_{12} - b_{21}a_{01})\right]\Big\}
\end{aligned}$$

where $\omega = \sqrt{-(a_{10}^2 + a_{01}b_{10})}$, which is guaranteed to be real since ω^2 is the determinant of the Jacobian matrix, which is positive at a Hopf bifurcation. (Those readers wondering why b_{01} does not appear in the above expressions are reminded that the Hopf bifurcation appears when the trace of the Jacobian matrix vanishes ($a_{10} + b_{01} = 0$), and hence b_{01} has been everywhere replaced by $-a_{10}$.) If, at the Hopf bifurcation, $L_1 < 0$, then the bifurcation is supercritical, with a stable equilibrium giving way to a stable limit cycle surrounding an unstable equilibrium. If instead $L_1 > 0$, then the bifurcation is subcritical, with an unstable limit cycle

surrounding a stable equilibrium giving way to an unstable equilibrium. (If $L_1 = 0$ there is a so-called Bautin bifurcation.)

We apply this approach to the rescaled system (11) with $u^* = 1 - \alpha\left(1-\delta^n\right)^{1/n}$, $v^* = u^*\left(1-\delta^n\right)^{1/n}/\delta$ and obtain the following coefficients:

$$a_{10} = 1 - 2u^* - \alpha p^{n+1}, \quad a_{01} = -\alpha\delta^{n+1}, \quad b_{10} = \beta p^{n+1}, \quad b_{01} = -\beta\delta(1-\delta^n),$$

$$a_{20} = -1 + \frac{n+1}{2}\,\alpha\delta^n p^{n+1}/u^*, \quad a_{02} = \frac{n+1}{2}\,\alpha\delta^{n+2}p^{n-1}/u^*,$$

$$a_{30} = -\frac{n+1}{6}\,\alpha\delta^n p^{n+1}[(n+2)\delta^n - (n-1)p^n]/u^{*2},$$

$$a_{21} = \frac{n+1}{2}\,\alpha\delta^{n+1}p^n[(n+1)\delta^n - np^n]/u^{*2},$$

$$a_{12} = -\frac{n+1}{2}\,\alpha\delta^{n+2}p^{n-1}[n\delta^n - (n+1)p^n]/u^{*2},$$

$$a_{03} = \frac{n+1}{6}\,\alpha\delta^{n+3}p^{n-2}[(n-1)\delta^n - (n+2)p^n]/u^{*2},$$

$$a_{11} = -(n+1)\alpha\delta^{n+1}p^n/u^*, \quad b_{11} = (n+1)\beta\delta^{n+1}p^n/u^*,$$

$$b_{20} = -\frac{n+1}{2}\,\beta\delta^n p^{n+1}/u^*, \quad b_{02} = -\frac{n+1}{2}\,\beta\delta^{n+2}p^{n-1}/u^*,$$

$$b_{30} = \frac{n+1}{6}\,\beta\delta^n p^{n+1}[(n+2)\delta^n - (n-1)p^n]/u^{*2},$$

$$b_{21} = -\frac{n+1}{2}\,\beta\delta^{n+1}p^n[(n+1)\delta^n - np^n]/u^{*2},$$

$$b_{12} = \frac{n+1}{2}\,\beta\delta^{n+2}p^{n-1}[n\delta^n - (n+1)p^n]/u^{*2},$$

$$b_{03} = -\frac{n+1}{6}\,\beta\delta^{n+3}p^{n-2}[(n-1)\delta^n - (n+2)p^n]/u^{*2},$$

where $p = \left(1-\delta^n\right)^{1/n}$. We then use the relation (10) for $\mathrm{tr}J(\check{E}_2) = 0$ to set one of the remaining parameter values, say

$$\beta = \frac{\alpha(1-\delta^n)^{1/n}(1+\delta^n) - 1}{\delta(1-\delta^n)},$$

and finally substitute values for n, α and δ to compute L_1.

We find, for instance, that for $n = 2$, $\delta = 0.4$ and $\alpha = 1$, $L_1 = 3.94565 > 0$, indicating a subcritical Hopf bifurcation, with an unstable limit cycle surrounding the LAS $\check{E}_2$ for β above the bifurcation point. Since for β below the bifurcation point there are no stable equilibria but solutions remain bounded, by Poincaré-Bendixson there must be a stable limit cycle around $\check{E}_2$. Since this stable limit cycle is not involved in the Hopf bifurcation, it must exist for β above the bifurcation point as well, surrounding the unstable limit cycle. Since for sufficiently high β $\check{E}_2$ is GAS, there must come a point at which the two limit cycles coalesce and disappear, in a saddle-node bifurcation of limit cycles. We find this same behavior for a range of values of n, δ and α, with $n > 1$, δ sufficiently small, and α sufficiently close to 1 for the Hopf bifurcation to occur. Figure 13 shows the (α, δ) plane divided into regions by the behavior around $\check{E}_2$ for $n = 2$.

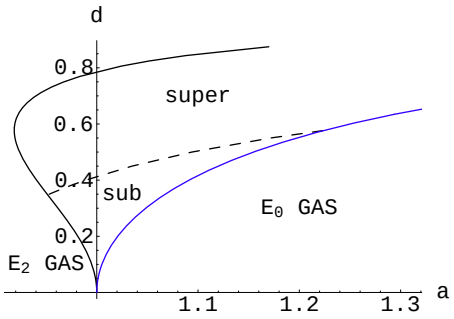

FIGURE 13. The (α, δ) parameter plane divided into regions by the behavior of system (8) around $\check{E}_2$ for $n = 2$. "Super" denotes the region where the Hopf bifurcation is supercritical; "sub" denotes the region where it is subcritical (and hence bistability occurs).

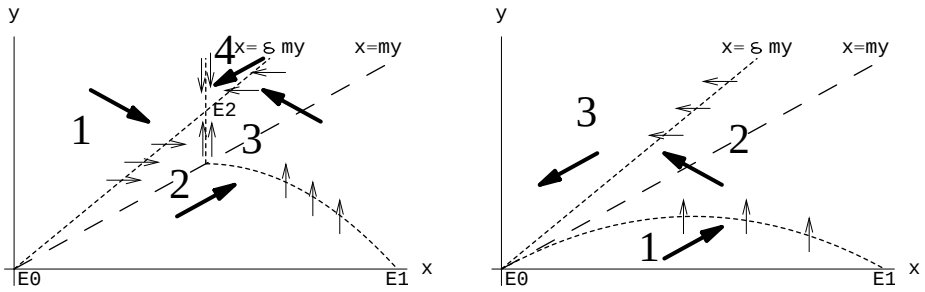

FIGURE 14. Phase portraits for system (9): (a) left, $\alpha < 1$; (b) right, $\alpha > 1$. Nullclines are dotted, and the switch line is dashed; arrows indicate vector field directions. Region numbers correspond to explanations in the main text.

System (9). On the side of the switch where $x < my$, the x-nullclines are $x = 0$ and $x/K = 1 - \alpha$, and the unique y-nullcline is the line $x = \delta my$ (note that since $\delta < 1$ this line always falls on the $x < my$ side of the switch), producing the equilibria E_0 and (when $\alpha < 1$) $\bar{E}_2$. A straightforward calculation of the Jacobian matrix in each case reveals that E_0 is LAS iff $\alpha > 1$, while $\bar{E}_2$ is LAS iff $\alpha < 1$.

On the side of the switch where $x > my$, the x-nullcline is the inverted parabola $y = \frac{r}{c}\, x \left(1 - \frac{x}{K}\right)$, and the y-nullcline is just $y = 0$, producing the equilibria E_0 and E_1. The Jacobian matrix evaluated at each equilibrium shows them both to be unstable.

To evaluate the switching behavior, we note that E_1 and $\bar{E}_2$ each fall on the correct respective sides of the switch to manifest in the composite model, while E_0 falls squarely on the switching line itself. E_0 is unstable for $x > my$, but for $\alpha > 1$ is LAS above the switching line, where $x < my$. The global behavior can be determined from the phase portraits, shown in Figure 14. It is straightforward to verify that solutions cannot grow unbounded in either case: $\limsup x$ is bounded by K, and consequently $\limsup y$ is bounded by $K/m\delta$.

When $\alpha > 1$, we can show the global asymptotic stability of E_0 in the switching model by observing that solutions beginning below the parabola $y = \frac{r}{c}\, x \left(1 - \frac{x}{K}\right)$

(region 1 in Figure 14(b)) eventually cross above it (to region 2) and do not return (since $dx/dt = 0$, $dy/dt > 0$ on it), that solutions beginning below the line $x = \delta my$ (region 2) eventually cross above it (to region 3) and do not return (since $dx/dt < 0$, $dy/dt > 0$ in the region just below it but $dx/dt < 0$, $dy/dt = 0$ on it), and that solutions above this line (region 3) move continually downward without crossing below it, thus inevitably approaching E_0.

When $\alpha < 1$, we can likewise show $\bar{E}_2$ to be GAS in (9) by observing an inevitable progression of any solution in region 1 of Figure 14(a) either toward $\bar{E}_2$ or into region 2, of any solution in region 2 either toward $\bar{E}_2$ or into region 3, of any solution in region 3 either toward $\bar{E}_2$ or into region 4, and finally of any solution in region 4 toward $\bar{E}_2$.

Received February 24, 2009; Accepted May 28, 2009.

E-mail address: kribs@uta.edu